Elzaki Transform Residual Power Series Method for the Fractional Population Diffusion Equations

Jianke Zhang, Xiaoyi Chen, Lifeng Li, Chang Zhou

***Abstract*—Residual power series method(RPSM) is an effective method for solving approximate analytic solutions of fractional differential equations(FDEs). However, the $(n-1)\alpha$ derivative of the residual function is required in this method. As we all know, it is difficult to compute the fractional-order derivative of a function by computer. This makes the application of the classic RPSM limited to a certain extent. To overcome the difficulty of the RPSM, we combine the Elzaki transform method with the RPSM to propose a new method, the Elzaki transform residual power series method(ERPSM). Firstly, the Elzaki transform is applied to both sides of the time FDEs. Secondly, the Elzaki inverse is taken on both sides of equation to obtain expression of the solution of the FDEs. Thirdly, the solution of the FDEs is expanded in fractional power series form and substituted into the equation. The unknown coefficient function is obtained by setting the residual function as zero and combining the initial conditions. Finally, the coefficient function is substituted into the power series form solution to obtain the finite term approximate analytic solutions. The new method is used to solve the time-fractional biological population diffusion equation(TFBPDEs). The presented results confirm the dependability and accuracy of the proposed method. This method does not require calculating the $(n-1)\alpha$ derivative of the residual function and is easy to be calculated on the computer. The ERPSM has less calculation effort than the classic RPSM. Some examples are given in datum and images, which are compared with the results of the RPSM and other methods.**

***Index Terms*—Residual power series method; Elzaki transform; Time-fractional biological population diffusion equations(TFBPDEs); Caputo derivative**

I. Introduction

THE fractional calculation's concept is debuted over 325 years, which was first proposed in 1695 by Leibniz and L'Hopital. FDEs have been widely applied in many areas, for instance, biological engineering, image processing[1], physical model[2] and risk analysis[3] etc. Nowadays, many researchers have proposed different methods to obtain approximate analytical solutions of FDEs, such as variational iteration method(VDM)[4], adomian decomposition method(ADM)[5], homotopy perturbation method(HPM)[6], modified generalized Taylor fractional series method[7], projected differential transform method[8] and so on.

Manuscript received March 15th, 2021; revised August 28th, 2021. This work is supported by the National Natural Science Foundation of China (Grant No.11701446), the Natural Science Foundation of Shaanxi Province (2020JM-577), New Star Team of Xi'an University of Posts and Telecommunications, Construction of Special Funds for Key Disciplines in Shaanxi Universities.

Jianke Zhang is an Associate Professor of the School of Science, Xi'an University of Posts and Telecommunications, Xi'an 710121, China.(e-mail:jiankezh@163.com).

Xiaoyi Chen is a student of the School of Science, Xi'an University of Posts and Telecommunications, Xi'an 710121, China.(e-mail:17629292134@163.com).

Lifeng Li is an Associate Professor of the School of Science, Xi'an University of Posts and Telecommunications, Xi'an 710121, China.(e-mail:lilifeng80@163.com).

Chang Zhou is an Associate Professor of the School of Science, Xi'an University of Posts and Telecommunications, Xi'an 710121, China.(e-mail:maytheday@163.com).

In the past few years, many scholars have been working on new methods for solving FDEs by the fractional RPSM. They applied these methods to solve analytical solutions of several classes of FDEs. In [9]-[14], many researchers have solved different types of FDEs using the RPSM. The RPSM is also used for many other problems, for example, the initial value problems [15], the fractional Zakharov-Kuznetsov equation [16], the time-fractional Fisher equation [17] and the high-order linear conformable fractional PDEs [18].

Elzaki transform modified from Laplace and Sumudu transform. In [19]-[21], Elzaki transform and other methods are combined to solve different differential equations.

In this paper, the Elzaki transform is combined with the RPSM, which is called ERPSM. Compared with the classic RPSM, fewer calculations can be obtained by the new method. The new method not only does not need to calculate the $(n-1)\alpha$ derivative of the residual function, but also can be easily implemented on the computer.

The general structure of this article is as follow. In section 2, the preliminaries of fractional order integrals, derivatives and Elzaki transform are presented. In section 3, ERPSM is proposed with the necessary fundamental procedure and the convergence analysis. In section 4, examples are given along with the corresponding numerical results and graphical conclusions. In the end, conclusions are drawn in section 5.

II. Preliminaries

In this section, the fundamental notion of the Caputo fractional and Elzaki transform are introduced systematically.

Definition 1 [22]. The Riemann-Liouville fractional integral operator of order $\alpha \geq 0$ is defined as

$$J^{\alpha}f(t)=\begin{cases} \frac{1}{\Gamma(\alpha)}\int_0^t \frac{f(s)}{(t-s)^{1-\alpha}}ds=\frac{1}{\Gamma(\alpha)}t^{\alpha-1}*f(t) & \alpha>0,t>0,\\ f(t) & \alpha=0,\end{cases} \quad (1)$$

where $t^{\alpha-1}*f(t)$ is the convolution product of $t^{\alpha-1}$ and $f(t)$.

For the Riemann-Liouville fractional integral, we have

1.$J^{\alpha}t^{\beta}=\frac{\Gamma(\beta+1)}{\Gamma(\beta+\alpha+1)}t^{\alpha+\beta}, \beta>-1$,

2.$J^{\alpha}(\lambda f(t)+\mu g(t))=\lambda J^{\alpha}f(t)+\mu J^{\alpha}g(t)$,

where λ and μ are real constants.

Definition 2 [23], [24]. Let $f(t):[0,+\infty)\to R$ be a function, and n be the upper positive integer of α $(\alpha>0)$. The Caputo fractional derivative is defined by

$$D^{\alpha}f(t)=\frac{1}{\Gamma(n-\alpha)}\int_0^t \frac{f^{(n)}(s)}{(t-s)^{\alpha+1-n}}ds, \quad n-1<\alpha\leq n, n\in N. \quad (2)$$

For the Caputo derivative, we have

$$1. D^{\alpha} J^{\alpha} f(t) = f(t),$$
$$2. J^{\alpha} D^{\alpha} f(t) = f(t) - \sum_{i=0}^{n-1} y^{(i)}(0)\frac{t^i}{i!},$$
$$3. D^{\alpha} t^{\beta} = \begin{cases} \frac{\Gamma(\beta+1)}{\Gamma(\beta+1-\alpha)} t^{\beta-\alpha} & \beta \geq \alpha \\ 0 & \beta < \alpha \end{cases},$$
$$4. D^{\alpha} c = 0,$$
$$5. D^{\alpha}(\lambda f(t) + \mu g(t)) = \lambda D^{\alpha} f(t) + \mu D^{\alpha} g(t),$$

where λ, μ and c are real constants.

Definition 3 [25]. A power series of the form

$$\sum_{m=0}^{\infty} f_m(x)(t-t_0)^{m\alpha} = f_0(x) + f_1(x)(t-t_0)^{\alpha} + f_2(t-t_0)^{2\alpha} + \cdots, 0 < n-1 < \alpha \leq n, t \geq t_0. \quad (3)$$

is called multiple fractional power series about $t = t_0$, where t is a variable and f_m's are functions of x called the coefficients of the series.

Theorem 1 [25]. Suppose that $u(x,t)$has a multiple fractional power series representation at $t = t_0$ of the form

$$u(x,t) = \sum_{m=0}^{\infty} u_m(x,t) = \sum_{m=0}^{\infty} f_m(x)(t-t_0)^{m\alpha}, \quad 0 < n-1 < \alpha \leq n, x \in I, t_0 \leq t < t_0 + R. \quad (4)$$

If $D_t^{m\alpha} u(x,t)$ are continuous on $I \times (t_0, t_0+R)$, $m = 0,1,2,\cdots$, then coefficients $f_m(x)$ of Eq. (4) are given as

$$f_m(x) = \frac{D_t^{m\alpha} u(x,t_0)}{\Gamma(m\alpha+1)}, m = 0,1,2,\cdots, \quad (5)$$

Where $D_t^{m\alpha} = \frac{\partial^{m\alpha}}{\partial t^{m\alpha}} = \frac{\partial^{\alpha}}{\partial t^{\alpha}} \cdot \frac{\partial^{\alpha}}{\partial t^{\alpha}} \cdots \frac{\partial^{\alpha}}{\partial t^{\alpha}} (m - times)$, and $R = min_{c \in I} R_c$, in which R_c is the radius of convergence of the fractional power series $\Sigma_{m=0}^{\infty} f_m(c)(t-t_0)^{m\alpha}$.

According to the convergence of the classic residual power series method, there is a real number $\lambda \in (0,1)$, such that $||u_m(x,t)|| \leq \lambda ||u_{m-1}(x,t)||$, $t \in (t_0, t_0+R)$.

Definition 4 [26], [27]. A new transform called the ELzaki transform defined for function of exponential order, we consider functions in the set A defined by:

$$A = f(t) : \exists M, k_1, k_2 > 0, |f(t)| < Me^{\frac{|t|}{kj}}, if t \in (-1)^j \times [0, \infty). \quad (6)$$

For a given function in the set, the constant M must be finite number, k_1, k_2 may be finite or infinite. The Elzaki transform which is defined by the integral equation

$$E[f(t)] = T(v) = v\int_0^{\infty} f(t) e^{\frac{-t}{v}} dt, t \geq 0, k_1 \leq v \leq k_2. \quad (7)$$

The following results can be obtained from the definition and simple calculations

1. $E[t^n] = n! v^{n+2}$,
2. $E[f'(t)] = \frac{T(v)}{v} - vf(0)$,
3. $E[f''(t)] = \frac{T(v)}{v^2} - f(0) - vf'(0)$,
4. $E[f^{(n)}(t)] = \frac{T(v)}{v^n} - \sum_{k=0}^{n-1} v^{2-n+k} f^{(k)}(0)$,
5. $E[t^{\alpha}] = \int_0^{\infty} e^{-vt} t^{\alpha} dt = v^{\alpha+1}\Gamma(\alpha+1), \mathbb{R}(\alpha) > 0$.

Theorem 2 [19]. If $T(v)$ is Elzaki transform of (t), one can consider the following Elzaki transform of the Riemann-Liouville derivative

$$E[D^{\alpha} f(t)] = v^{-\alpha}[T(v) - \sum_{k=1}^{n} v^{\alpha-k+2}[D^{\alpha-k} f(0)]]; \quad -1 < n-1 \leq \alpha < n. \quad (8)$$

Definition 5 [19]. The Elzaki transform of the Caputo fractional derivative by using Theorem 2 is defined as follows

$$E[D^{\alpha} f(t)] = v^{-\alpha} E[f(t)] - \Sigma_{k=0}^{m-1} v^{2-\alpha+k} f^{(k)}(0), \quad (9)$$

where $m - 1 < \alpha < m$.

III. Direct method of ERPSM

In this chapter, steps of the ERPSM are presented. The new method combines the Elzaki transform with the RPSM to solve the TFBPDEs, which is based on the classic RPSM. In this segment, we consider the TFBPDEs is

$$D_t^{\alpha} u(x,y,t) = (u^2(x,y,t))_{xx} + (u^2(x,y,t))_{yy} + \sigma(u(x,y,t)), \quad t > 0, x, y \in \mathbb{R}$$

$$u(x,y,0) = f(x,y), \quad (10)$$

where u indicates the population density, $\sigma(u)$ indicates the births and deaths of the population. Also, $\sigma(u) = hu^a(1 - ru^b)$ with h, a, r, b are real numbers[28].

In this section, steps and the necessary definitions are given, and we set up a general form of a nonlinear inhomogeneous partial differential equation. The form is

$$D_t^{\alpha} u(x,y,t) = \mathcal{L}(u(x,y,t)) + \mathcal{N}(u(x,y,t)) + \sigma(u(x,y,t)), \quad (11)$$

with

$$u_i(x,y,t)|_{t=0} = g_k, k = 0, \ldots, n-1, \quad (12)$$

where σ is a known function, $\mathcal{N}$ is the general nonlinear fraction differential operator and $\mathcal{L}$ represents a linear fraction differential operator.

We propose some steps for the ERPSM as follows

Step 1. Using Elzaki transform on both sides of the equation, the form is

$$E[D_t^{\alpha} u(x,y,t)] = E[\mathcal{L}(u(x,y,t)) + \mathcal{N}(u(x,y,t)) + \sigma(u(x,y,t))], \quad (13)$$

Applying the differentiation property of Elzaki transform and the initial conditions above, we can obtain

$$E[u(x,y,t)] = g(x,y,t) + v^{\alpha} E[\mathcal{L}(u(x,y,t)) + \mathcal{N}(u(x,y,t)) + \sigma(u(x,y,t))]. \quad (14)$$

Step 2. Taking Elzaki inverse on both sides of the equation

$$u(x,y,t) = G(x,y,t) + E^{-1}[v^{\alpha} E[\mathcal{L}(u(x,y,t)) + \mathcal{N}(u(x,y,t)) + \sigma(u(x,y,t))]], \quad (15)$$

where $G(x,y,t)$ represents the initial condition.

Step 3. We use the classic RPSM, the algorithm can be proposed by

$$u(x,y,t) = \sum_{n=0}^{\infty} f_n(x,y) \frac{t^{n\alpha}}{\Gamma(1+n\alpha)}, \quad (16)$$

To obtain the approximate value of (16), the form of $u_i(x,y,t)$ can be written as

$$S_i=\sum_{n=0}^{i}u_n(x,y,t)=\sum_{n=0}^{i}f_n(x,y)\frac{t^{n\alpha}}{\Gamma(1+n\alpha)}. \tag{17}$$

Step 4. We combine Step 2 with Step 3, we can attain

$$Res_i(x,y,t)=u_i(x,y,t)-\{G(x,y,t)+E^{-1}[v^\alpha E[\mathcal{L}(u_{i-1}(x,y,t))+\mathcal{N}(u_{i-1}(x,y,t))+\sigma(u_{i-1}(x,y,t))]]\}, \tag{18}$$

Then,

$$Res_n(x,y,t)|_{t=0}=0,\quad n\in N^*, \tag{19}$$

to find the result of $f_n(x,y)(n\in N^*)$, where $Res_n(x,y,t)$ is the residual function of equation (11).

Here, ERPSM will give the i^{th}-order approximate solutions with

$$S_i=u_0+u_1+u_2+\ldots+u_i, \tag{20}$$

where

$$\begin{aligned}u_0&=f_0(x,y),\\ u_1&=f_1(x,y)\frac{t^\alpha}{\Gamma(1+\alpha)},\\ u_2&=f_2(x,y)\frac{t^{2\alpha}}{\Gamma(1+2\alpha)},\\ &\vdots\\ u_i&=f_i(x,y)\frac{t^{i\alpha}}{\Gamma(1+i\alpha)}.\end{aligned} \tag{21}$$

Remark Generally, for any $\alpha\in(0,1]$, $|\tilde{Res}(x,y,t)|_{exact}$ equals zero. We can use the value of $|\tilde{Res}_i(x,y,t)|$ to indicate the deviation between the approximate solution and the exact solution. The form of $|\tilde{Res}_i(x,y,t)|$ can be defined as

$$|\tilde{Res}_i(x,y,t)|=|D_t^\alpha u_i(x,y,t)-(u_i^2(x,y,t))_{xx}-(u_i^2(x,y,t))_{yy}-\sigma u_i(x,y,t)| \tag{22}$$

IV. Illustrative examples

In this subsection, examples are settled by ERPSM. We usually compute the initial iteration in the new way and ignore the rest. Then the Elzaki transform method is applied, we obtain the unknown coefficients. We analyze the approximate solutions by charts and graphics.

Example 1 With $a=1,r=0$, considering the following TFBPDEs

$$D_t^\alpha u(x,y,t)=(u^2(x,y,t))_{xx}+(u^2(x,y,t))_{yy}+hu(x,y,t),\quad t>0,0<\alpha\le1, \tag{23}$$

with

$$u(x,y,t)|_{t=0}=\sqrt{xy}, \tag{24}$$

Using Elzaki transform

$$E[D_t^\alpha u(x,y,t)]=E[(u^2(x,y,t))_{xx}+(u^2(x,y,t))_{yy}+hu(x,y,t)], \tag{25}$$

Applying the differentiation property of Elzaki transform and the initial conditions above, we can obtain

$$E[u(x,y,t)]=g(x,y,t)+v^\alpha E[(u^2(x,y,t))_{xx}+(u^2(x,y,t))_{yy}+h(x,y,t)]. \tag{26}$$

Taking Elzaki inverse

$$u(x,y,t)=G(x,y,t)+E^{-1}[v^\alpha E[(u^2(x,y,t))_{xx}+(u^2(x,y,t))_{yy}+hu(x,y,t)]], \tag{27}$$

We use the classic RPSM. The form of $u_i(x,y,t)$ can be written as

$$S_i=\sum_{n=0}^{i}u_n(x,y,t)=\sum_{n=0}^{i}f_n(x,y)\frac{t^{n\alpha}}{\Gamma(1+n\alpha)}. \tag{28}$$

Then, we find the solution of $f_n(x,y)$ by

$$Res_i(x,y,t)=u_i(x,y,t)-\{G(x,y,t)+E^{-1}[v^\alpha E[(u_{i-1}^2(x,y,t))_{xx}+(u_{i-1}^2(x,y,t))_{yy}+hu_{i-1}(x,y,t)]]\}. \tag{29}$$

When $i=0$

$$Res_0(x,y,t)=u_0(x,y,t)-G(x,y,t),$$

and from the equation (17), we have

$$u_0(x,y,t)=f_0(x,y),$$

from formula (19), we have $Res_0(x,y,t)|_{t=0}=0$, thus

$$f_0(x,y)=\sqrt{xy}. \tag{30}$$

When $i=1$

$$Res_1(x,y,t)=u_1(x,y,t)-\{G(x,y,t)+E^{-1}[v^\alpha E[(u_0^2(x,y,t))_{xx}+(u_0^2(x,y,t))_{yy}+hu_0(x,y,t)]]\},$$

with the condition

$$u_1(x,y,t)=f_0(x,y)+f_1(x,y)\frac{t^\alpha}{\Gamma(1+\alpha)},$$

Then, we can attain

$$\begin{aligned}&Res_1(x,y,t)\\ &=f_0(x,y)+f_1(x,y)\frac{t^\alpha}{\Gamma(1+\alpha)}-\{G(x,y,t)\\ &+E^{-1}[v^\alpha E[(f_0^2(x,y))_{xx}+(f_0^2(x,y))_{yy}+hf_0(x,y)]]\}\\ &=f_1(x,y)\frac{t^\alpha}{\Gamma(1+\alpha)}-E^{-1}[v^\alpha E[h\sqrt{xy}]]\\ &=f_1(x,y)\frac{t^\alpha}{\Gamma(1+\alpha)}-E^{-1}[h\sqrt{xy}v^{\alpha+2}]\\ &=f_1(x,y)\frac{t^\alpha}{\Gamma(1+\alpha)}-\frac{h\sqrt{xy}t^\alpha}{\Gamma(1+\alpha)},\end{aligned}$$

Then, we solve $t^{-\alpha}Res_1(x,y,t)|_{t=0}=0$ to obtain

$$f_1(x,y)=h\sqrt{xy}. \tag{31}$$

When $i=2$

$$Res_2(x,y,t)=u_2(x,y,t)-\{G(x,y,t)+E^{-1}[v^\alpha E[(u_1^2(x,y,t))_{xx}+(u_1^2(x,y,t))_{yy}+hu_1(x,y,t)]]\},$$

with the condition

$$u_2(x,y,t)=f_0(x,y)+f_1(x,y)\frac{t^\alpha}{\Gamma(1+\alpha)}+f_2(x,y)\frac{t^{2\alpha}}{\Gamma(1+2\alpha)},$$

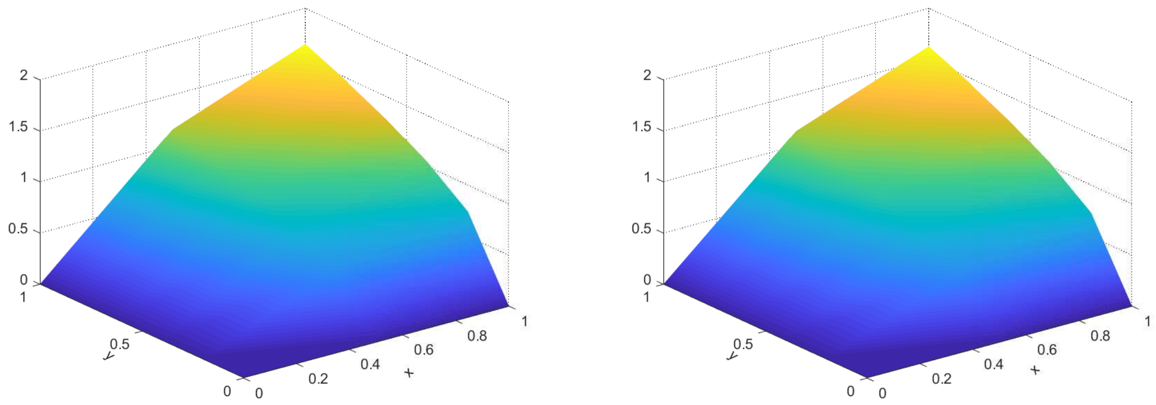

(a) $u(x,y,t)_{exact}$ (b) $u(x,y,t)_{ERPSM}$

Fig. 1: 3D graphics of exact and approximate solutions(Ex. 1.)

TABLE I: The absolute errors of ERPSM, RPSM, HPM for $\alpha = 1$ and $t = 1$(Ex. 1.)

x	y	$u(x,y,t)_{exact}$	$u_i(x,y,t)_{i=2}^{ERPSM}$	$Error(x,y,t)_{i=2}^{RPSM}$[30]	$Error(x,y,t)_{i=2}^{ERPSM}$	$Error(x,y,t)_{i=2}^{HPM}$[30]
	0.1	0.1648721271	0.1625000000	2.37×10^{-3}	2.37×10^{-3}	2.37×10^{-3}
	0.2	0.2331643981	0.2298097038	3.35×10^{-3}	3.35×10^{-3}	3.35×10^{-3}
0.1	0.3	0.2855669010	0.2814582563	4.11×10^{-3}	4.11×10^{-3}	4.11×10^{-3}
	0.4	0.3297442542	0.3250000000	4.74×10^{-3}	4.74×10^{-3}	4.74×10^{-3}
	0.5	0.3686652837	0.3633610463	5.30×10^{-3}	5.30×10^{-3}	5.30×10^{-3}
	0.1	0.2855669010	0.2814582563	4.11×10^{-3}	4.11×10^{-3}	4.11×10^{-3}
	0.2	0.4038525842	0.3980420832	5.81×10^{-3}	5.81×10^{-3}	5.81×10^{-3}
0.3	0.3	0.4946163813	0.4875000000	7.12×10^{-3}	7.12×10^{-3}	7.12×10^{-3}
	0.4	0.5711338018	0.5629165124	8.22×10^{-3}	8.22×10^{-3}	8.22×10^{-3}
	0.5	0.6385470025	0.6293597937	9.19×10^{-3}	9.19×10^{-3}	9.19×10^{-3}
	0.1	0.3686652837	0.3633610463	5.30×10^{-3}	5.30×10^{-3}	5.30×10^{-3}
	0.2	0.5213714443	0.5138701198	7.50×10^{-3}	7.50×10^{-3}	7.50×10^{-3}
0.5	0.3	0.6385470025	0.6293597937	9.19×10^{-3}	9.19×10^{-3}	9.19×10^{-3}
	0.4	0.7373305676	0.7267220927	1.06×10^{-2}	1.06×10^{-2}	1.06×10^{-2}
	0.5	0.8243606355	0.8125000000	1.19×10^{-2}	1.19×10^{-2}	1.19×10^{-2}
	0.1	0.5213714443	0.5138701198	7.50×10^{-3}	7.50×10^{-3}	7.50×10^{-3}
	0.2	0.7373305676	0.7267220927	1.06×10^{-2}	1.06×10^{-2}	1.06×10^{-2}
1	0.3	0.9030418312	0.8900491559	1.30×10^{-2}	1.30×10^{-2}	1.30×10^{-2}
	0.4	1.0427428890	1.0277402400	1.50×10^{-2}	1.50×10^{-2}	1.50×10^{-2}
	0.5	1.1658219910	1.1490485190	1.68×10^{-2}	1.68×10^{-2}	1.68×10^{-2}

TABLE II: The values of $\mid \tilde{Res}(x,y,t) \mid$ by ERPSM,RPSM,HPM for $\alpha = 0.3, 0.6$ and $t = 0.1(Ex1.)$

		$\alpha = 0.3$				$\alpha = 0.6$			
x	y	$u_i(x,y,t)_{i=2}^{ERPSM}$	$\lvert\tilde{Res}\rvert_{ERPSM}$	$\lvert\tilde{Res}\rvert_{RPSM}$[30]	$\lvert\tilde{Res}\rvert_{HPM}$[30]	$u_i(x,y,t)_{i=2}^{ERPSM}$	$\lvert\tilde{Res}\rvert_{ERPSM}$	$\lvert\tilde{Res}\rvert_{RPSM}$[30]	$\lvert\tilde{Res}\rvert_{HPM}$[30]
	0.1	0.119	7.590×10^{-4}	7.590×10^{-4}	7.590×10^{-4}	0.131	1.546×10^{-4}	1.546×10^{-4}	1.546×10^{-4}
0.1	0.2	0.169	1.073×10^{-3}	1.073×10^{-3}	1.073×10^{-3}	0.185	2.187×10^{-4}	2.187×10^{-4}	2.187×10^{-4}
	0.3	0.207	1.315×10^{-3}	1.315×10^{-3}	1.315×10^{-3}	0.226	2.678×10^{-4}	2.678×10^{-4}	2.678×10^{-4}
	0.1	0.169	1.073×10^{-3}	1.073×10^{-3}	1.073×10^{-3}	0.185	2.187×10^{-4}	2.187×10^{-4}	2.187×10^{-4}
0.2	0.2	0.239	1.518×10^{-3}	1.518×10^{-3}	1.518×10^{-3}	0.261	$3,092 \times 10^{-4}$	3.092×10^{-4}	3.092×10^{-4}
	0.3	0.292	1.859×10^{-3}	1.859×10^{-3}	1.859×10^{-3}	0.320	3.787×10^{-4}	3.787×10^{-4}	3.787×10^{-4}
	0.1	0.207	1.315×10^{-3}	1.315×10^{-3}	1.315×10^{-3}	0.226	2.678×10^{-4}	2.678×10^{-4}	2.678×10^{-4}
0.3	0.2	0.292	1.859×10^{-3}	1.859×10^{-3}	1.859×10^{-3}	0.320	3.787×10^{-4}	3.787×10^{-4}	3.787×10^{-4}
	0.3	0.358	2.277×10^{-3}	2.277×10^{-3}	2.277×10^{-3}	0.392	4.639×10^{-4}	4.639×10^{-4}	4.639×10^{-4}

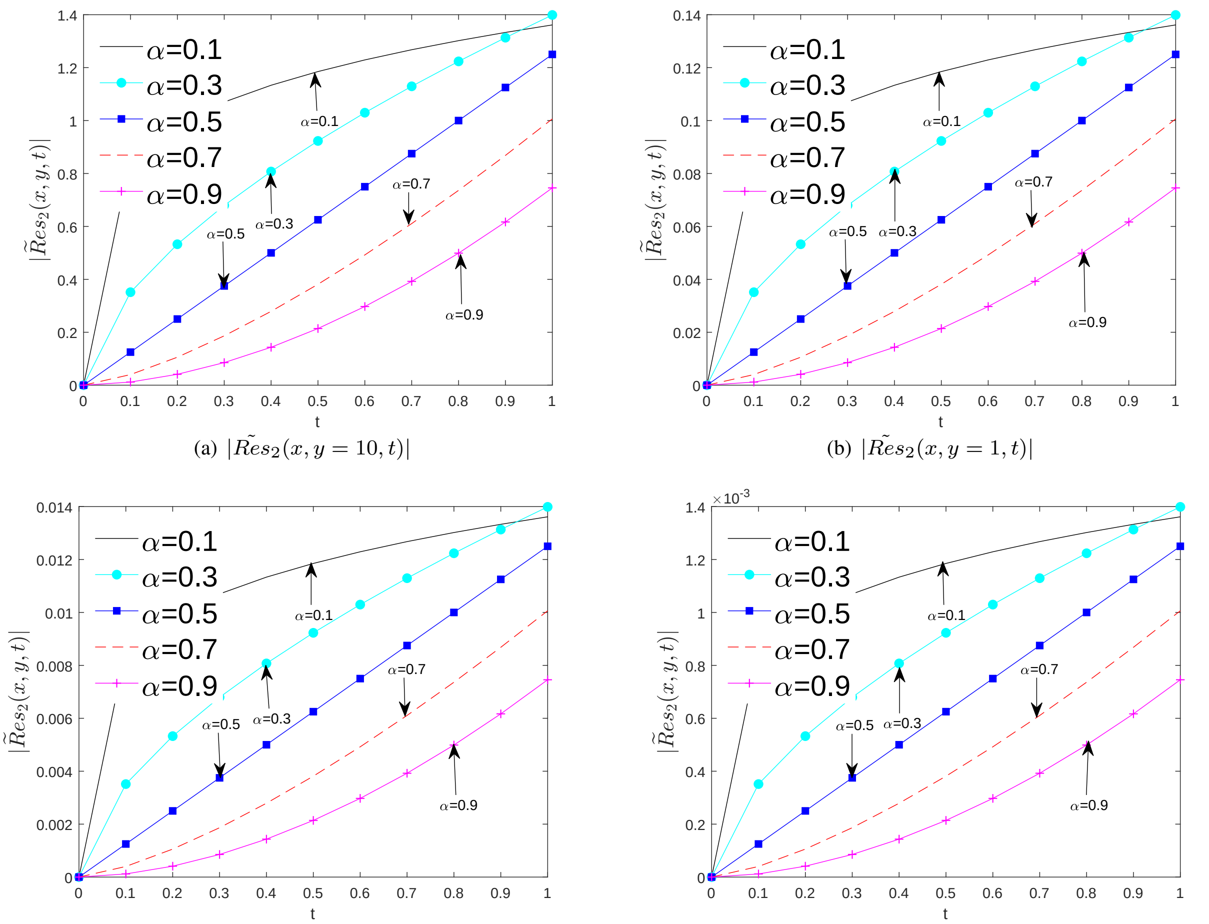

(a) $|\tilde{Res}_2(x, y = 10, t)|$ (b) $|\tilde{Res}_2(x, y = 1, t)|$

(c) $|\tilde{Res}_2(x, y = 0.1, t)|$ (d) $|\tilde{Res}_2(x, y = 0.01, t)|$

Fig. 2: $|\tilde{Res}_2(x, y, t)|$ with different t and α(Ex. 1.)

Then, we can get

$$\begin{aligned}
&Res_2(x,y,t)\\
&=f_0(x,y)+f_1(x,y)\frac{t^\alpha}{\Gamma(1+\alpha)}+f_2(x,y)\frac{t^{2\alpha}}{\Gamma(1+2\alpha)}\\
&-\{G(x,y,t)+E^{-1}[v^\alpha E[((f_0(x,y)+f_1(x,y)\frac{t^\alpha}{\Gamma(1+\alpha)})^2)_{xx}\\
&+((f_0(x,y)+f_1(x,y)\frac{t^\alpha}{\Gamma(1+\alpha)})^2)_{yy}+h(f_0(x,y)\\
&+f_1(x,y)\frac{t^\alpha}{\Gamma(1+\alpha)})]]\}\\
&=f_1(x,y)\frac{t^\alpha}{\Gamma(1+\alpha)}+f_2(x,y)\frac{t^{2\alpha}}{\Gamma(1+2\alpha)}\\
&-E^{-1}[v^\alpha E[h\sqrt{xy}]]-E^{-1}[v^\alpha E[h^2\sqrt{xy}v^{\alpha+2}]]\\
&=f_1(x,y)\frac{t^\alpha}{\Gamma(1+\alpha)}+f_2(x,y)\frac{t^{2\alpha}}{\Gamma(1+2\alpha)}\\
&-E^{-1}[h\sqrt{xy}v^{\alpha+2}]-E^{-1}[h^2\sqrt{xy}v^{2\alpha+2}]\\
&=f_1(x,y)\frac{t^\alpha}{\Gamma(1+\alpha)}+f_2(x,y)\frac{t^{2\alpha}}{\Gamma(1+2\alpha)}\\
&-\frac{h\sqrt{xy}t^\alpha}{\Gamma(1+\alpha)}-\frac{h^2\sqrt{xy}t^{2\alpha}}{\Gamma(1+2\alpha)},
\end{aligned}$$

Thereby, from $t^{-2\alpha}Res_2(x,y,t)|_{t=0} = 0$, we get

$$f_2(x,y) = h^2\sqrt{xy}. \quad (32)$$

We can get an approximate result

$$u_2(x,y,t)=\sqrt{xy}+h\sqrt{xy}\frac{t^\alpha}{\Gamma(1+\alpha)}+h^2\sqrt{xy}\frac{t^{2\alpha}}{\Gamma(1+2\alpha)}. \quad (33)$$

Therefore, the n-th coefficient of $u(x,y,t)$ is

$$f_n(x,y) = h^n\sqrt{xy}, \quad (34)$$

the n-th ERPSM approximate solutions of $u(x,y,t)$ is

$$u_n(x,y,t) = \sqrt{xy}\sum_{n=0}^{i}\frac{(ht^\alpha)^n}{\Gamma(1+n\alpha)}, \quad (35)$$

and as $n \to \infty$ we have

$$u(x,y,t) = lim_{n\to\infty}u_n(x,y,t) = \sqrt{xy}E_\alpha(ht^\alpha), \quad (36)$$

where $E_\alpha(z)$ is the Mittag-Leffler function defined as $E_\alpha(z) = \Sigma_{n=0}^{i}\frac{z^n}{\Gamma(1+n\alpha)}$[29]. Obviously, when $\alpha \to 1$, we have $E_\alpha(z) = e^{ht}$ and hence $\sqrt{xy}e^{ht}$ is the exact solution of the standard partial time-derivative of (23).

In Fig. 1, we obtain the 3D graphics of the approximate solutions and exact solutions by Matlab 2018b Windows(64 bit). The approximate solutions are the same as the exact solutions. The parameters in Fig. 1 are $\alpha = 1, t = 1, h = 0.5$, where Fig. 1(a) represents the exact solutions and Fig. 1(b) represents the approximate solutions.

The absolute error is

$$Error(x,y,t) = \mid u(x,y,t)_{exact} - u_i(x,y,t)_{ERPSM} \mid . \quad (37)$$

For the items in the table, the front part is the required parameters and the back part is the required result, where the upper right corner is the method name and the lower right corner is the number of terms expanded by the method

In Tab. 1, we show the absolute error of three methods when $h = 0.5$. The three methods are the ERPSM, the classic RPSM[30] and the HPM[6]. Besides, the ERPSM is denoted by $u_i(x,y,t)$, the RPSM and HPM are denoted by $\tilde{u}_i(x,y,t)$. The approximate solutions of HPM and classic RPSM for $i = 2$ can be written as

$$\tilde{u}_2(x,y,t) = \sqrt{xy} + \frac{ht^\alpha}{\Gamma(1+\alpha)}\sqrt{xy} + \frac{h^2 t^{2\alpha}}{\Gamma(1+2\alpha)}\sqrt{xy}. \quad (38)$$

In Tab. 1, under the same conditions, although the absolute error values were obtained by the ERPSM, the classic RPSM and the HPM are the same, the new method requires less computation.

When $\alpha = 0.1, 0.3, 0.5, 0.7, 0.9$, linear independence can be verified by using the ERPSM. Then, we use the Elzaki transform method to attain the unknown coefficients.

In Fig. 2, pictures show the impact of different α and x, y when $h = 0.5, t \in [0,1], x \in (0,10], y \in (0,10]$ on the $|\tilde{Res}_2(x,y,t)|$. We list four cases of fixed x, y to observe the variation of $|\tilde{Res}_2(x,y,t)|$ in each subplot with different α and t. Different colors and line shapes represent different α. Fig. 2(a)-2(d) respectively show $|\tilde{Res}_2(x,y,t)|$ of x, y are fixed values of 10, 1, 0.1 and 0.01.

We can draw a conclusion from Fig. 2 that $|\tilde{Res}_2(x,y,t)|$ decreases as the constants x, y decreases when α and t are unchanged. Besides, $|\tilde{Res}_2(x,y,t)|$ decreases as α increases when t and x, y are unchanged, $|\tilde{Res}_2(x,y,t)|$ increases as $t \in (0,1)$ increases when α and x, y are unchanged. From Fig. 2(a)-2(d), $|\tilde{Res}_2(x,y,t)|$ is a constant. Moreover, when $t \to 0$, $|\tilde{Res}_2(x,y,t)| \to 0$, which is because $u_2(x,y,t)$ is a generalized Taylor expansion at $t_0 = 0$. If $t \to 0$, the precision of $u_2(x,y,t)$ is higher.

Using the ERPSM, when $\alpha = 0.3, 0.6$, the linearly independence can be verified. Then, we use the Elzaki transform method to attain the unknown coefficients. In Tab. 2, we show the approximate solutions and the values of $\mid \tilde{Res}(x,y,t) \mid$ when $t = 0.1, h = 0.3, i = 2$.

Example 2 With $a = 1, b = 1$, considering the following TFBPDEs

$$\begin{aligned} D_t^\alpha u(x,y,t) &= (u^2(x,y,t))_{xx} + (u^2(x,y,t))_{yy} \\ &+ hu(x,y,t)(1-ru(x,y,t)), t > 0, 0 < \alpha \le 1, \end{aligned} \quad (39)$$

with

$$u(x,y,t)|_{t=0} = e^{\sqrt{\frac{hr}{8}}(x+y)}, \quad (40)$$

Using Elzaki transform

$$\begin{aligned} E[D_t^\alpha u(x,y,t)] &= E[(u^2(x,y,t))_{xx} + (u^2(x,y,t))_{yy} \\ &+ h(x,y,t)(1-ru(x,y,t))], \end{aligned} \quad (41)$$

Applying the differentiation property of Elzaki transform and the initial conditions above, we can obtain

$$\begin{aligned} E[u(x,y,t)] &= g(x,y,t) + v^\alpha E[(u^2(x,y,t))_{xx} \\ &+ (u^2(x,y,t))_{yy} + h(x,y,t)(1-ru(x,y,t))]. \end{aligned} \quad (42)$$

Taking Elzaki inverse

$$\begin{aligned} u(x,y,t) &= G(x,y,t) + E^{-1}[v^\alpha E[(u^2(x,y,t))_{xx} \\ &+ (u^2(x,y,t))_{yy} + hu(x,y,t)(1-ru(x,y,t))]]. \end{aligned} \quad (43)$$

We use the classic RPSM. The form of $u_i(x,y,t)$ can be written as

$$S_i = \sum_{n=0}^{i} u_n(x,y,t) = \sum_{n=0}^{i} f_n(x,y)\frac{t^{n\alpha}}{\Gamma(1+n\alpha)}. \quad (44)$$

Then, we find the solution of $f_n(x,y)$ by

$$\begin{aligned} Res_i(x,y,t) &= u_i(x,y,t) - \{G(x,y,t) \\ &+ E^{-1}[v^\alpha E[(u_{i-1}^2(x,y,t))_{xx} + (u_{i-1}^2(x,y,t))_{yy} \\ &+ hu_{i-1}(x,y,t)(1-ru_{i-1}(x,y,t))]]\}. \end{aligned} \quad (45)$$

When $i = 0$

$$Res_0(x,y,t) = u_0(x,y,t) - G(x,y,t),$$

and from the equation (17), we have

$$u_0(x,y,t) = f_0(x,y),$$

from formula (19), we have $Res_0(x,y,t)|_{t=0} = 0$, thus

$$f_0(x,y) = e^{\sqrt{\frac{hr}{8}}(x+y)}. \quad (46)$$

When $i = 1$

$$\begin{aligned} Res_1(x,y,t) &= u_1(x,y,t) - \{G(x,y,t) \\ &+ E^{-1}[v^\alpha E[(u_0^2(x,y,t))_{xx} + (u_0^2(x,y,t))_{yy} \\ &+ hu_0(x,y,t)(1-ru_0(x,y,t))]]\}. \end{aligned}$$

with the condition

$$u_1(x,y,t) = f_0(x,y) + f_1(x,y)\frac{t^\alpha}{\Gamma(1+\alpha)},$$

Then, we can attain

$$\begin{aligned} &Res_1(x,y,t) \\ &= f_0(x,y) + f_1(x,y)\frac{t^\alpha}{\Gamma(1+\alpha)} - \{G(x,y,t) \\ &+ E^{-1}[v^\alpha E[(f_0^2(x,y))_{xx} + (f_0^2(x,y))_{yy} \\ &+ hf_0(x,y)(1-rf_0(x,y))]]\} \\ &= f_1(x,y)\frac{t^\alpha}{\Gamma(1+\alpha)} - E^{-1}[v^\alpha E[he^{\sqrt{\frac{hr}{8}}(x+y)}]] \\ &= f_1(x,y)\frac{t^\alpha}{\Gamma(1+\alpha)} - E^{-1}[he^{\sqrt{\frac{hr}{8}}(x+y)}v^{\alpha+2}] \\ &= f_1(x,y)\frac{t^\alpha}{\Gamma(1+\alpha)} - \frac{he^{\sqrt{\frac{hr}{8}}(x+y)}t^\alpha}{\Gamma(1+\alpha)}, \end{aligned}$$

Then, we solve $t^{-\alpha}Res_1(x,y,t)|_{t=0} = 0$ to obtain

$$f_1(x,y) = he^{\sqrt{\frac{hr}{8}}(x+y)}. \quad (47)$$

When $i = 2$

$$\begin{aligned} Res_2(x,y,t) &= u_2(x,y,t) - \{G(x,y,t) \\ &+ E^{-1}[v^\alpha E[(u_1^2(x,y,t))_{xx} + (u_1^2(x,y,t))_{yy} \\ &+ hu_1(x,y,t)(1-ru_1(x,y,t))]]\}, \end{aligned}$$

with the condition

$$u_2(x,y,t) = f_0(x,y) + f_1(x,y)\frac{t^\alpha}{\Gamma(1+\alpha)} + f_2(x,y)\frac{t^{2\alpha}}{\Gamma(1+2\alpha)},$$

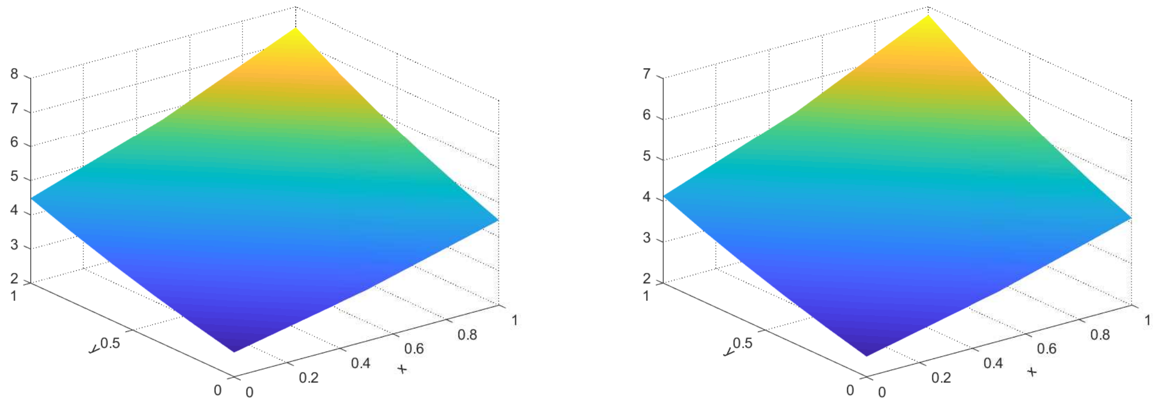

(a) $u(x, y, t)_{exact}$ (b) $u(x, y, t)_{ERPSM}$

Fig. 3: 3D graphics of exact and approximate solutions(Ex. 2.)

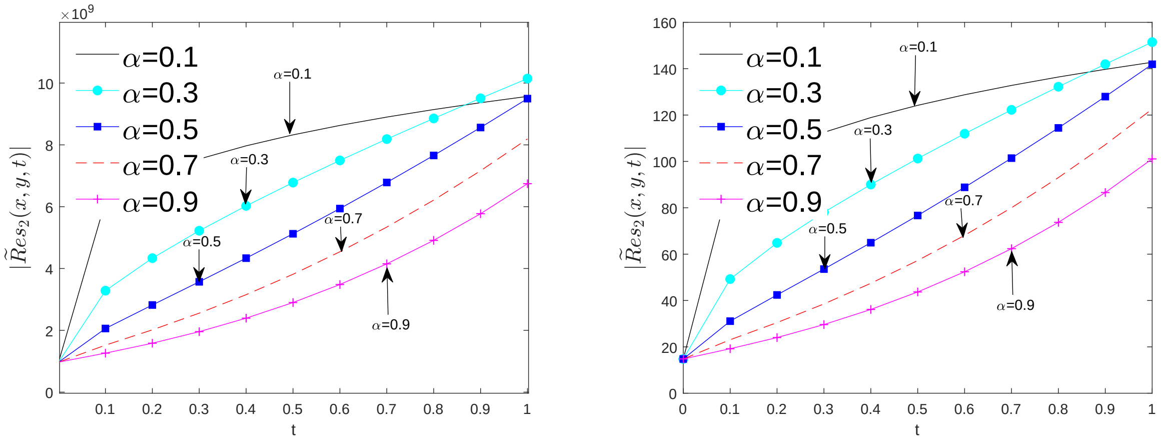

(a) $|\tilde{Res}_2(x, y = 10, t)|$ (b) $|\tilde{Res}_2(x, y = 1, t)|$

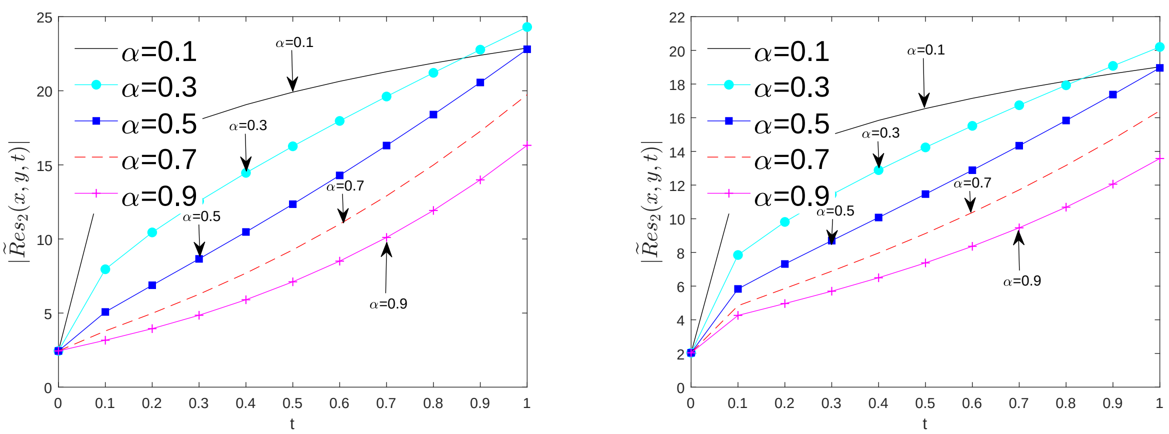

(c) $|\tilde{Res}_2(x, y = 0.1, t)|$ (d) $|\tilde{Res}_2(x, y = 0.01, t)|$

Fig. 4: $|\tilde{Res}_2(x, y, t)|$ with different t and α(Ex. 2.)

TABLE III: Absolute errors by ERPSM for $\alpha = 1$(Ex. 2.)

	$Error(x,y,t)_{i=2}^{EPRSM}$				
t/x,y	0.1	0.3	0.5	0.7	0.9
0.1	0.000188894	0.000230715	0.000281796	0.000344187	0.000420390
0.3	0.005369813	0.006558703	0.008010819	0.009784437	0.011950739
0.5	0.026216058	0.032020365	0.039109763	0.047768774	0.058344912
0.7	0.075983492	0.092806446	0.113354051	0.138450952	0.169104373
0.9	0.170862862	0.208692371	0.254897437	0.311332434	0.380262293

Then, we can get

$$
\begin{aligned}
&Res_2(x,y,t)\\
&= f_0(x,y)+f_1(x,y)\frac{t^\alpha}{\Gamma(1+\alpha)}+f_2(x,y)\frac{t^{2\alpha}}{\Gamma(1+2\alpha)}\\
&-\{G(x,y,t)+E^{-1}[v^\alpha E[((f_0(x,y)+f_1(x,y)\frac{t^\alpha}{\Gamma(1+\alpha)})^2)_{xx}\\
&+((f_0(x,y)+f_1(x,y)\frac{t^\alpha}{\Gamma(1+\alpha)})^2)_{yy}+h(f_0(x,y)\\
&+f_1(x,y)\frac{t^\alpha}{\Gamma(1+\alpha)})(1-r(f_0(x,y)+f_1(x,y)\frac{t^\alpha}{\Gamma(1+\alpha)}))]]\}\\
&= f_1(x,y)\frac{t^\alpha}{\Gamma(1+\alpha)}+f_2(x,y)\frac{t^{2\alpha}}{\Gamma(1+2\alpha)}\\
&-E^{-1}[v^\alpha E[he^{\sqrt{\frac{hr}{8}}(x+y)}]]-E^{-1}[v^\alpha E[h^2e^{\sqrt{\frac{hr}{8}}(x+y)}v^{\alpha+2}]]\\
&= f_1(x,y)\frac{t^\alpha}{\Gamma(1+\alpha)}+f_2(x,y)\frac{t^{2\alpha}}{\Gamma(1+2\alpha)}\\
&-E^{-1}[he^{\sqrt{\frac{hr}{8}}(x+y)}v^{\alpha+2}]-E^{-1}[h^2e^{\sqrt{\frac{hr}{8}}(x+y)}v^{2\alpha+2}]\\
&= f_1(x,y)\frac{t^\alpha}{\Gamma(1+\alpha)}+f_2(x,y)\frac{t^{2\alpha}}{\Gamma(1+2\alpha)}\\
&-\frac{he^{\sqrt{\frac{hr}{8}}(x+y)}t^\alpha}{\Gamma(1+\alpha)}-\frac{h^2e^{\sqrt{\frac{hr}{8}}(x+y)}t^{2\alpha}}{\Gamma(1+2\alpha)},
\end{aligned}
$$

Thereby, from $t^{-2\alpha}Res_2(x,y,t)|_{t=0} = 0$, we get

$$f_2(x,y) = h^2 e^{\sqrt{\frac{hr}{8}}(x+y)}. \tag{48}$$

We can get an approximate result

$$
\begin{aligned}
u_2(x,y,t) = e^{\sqrt{\frac{hr}{8}}(x+y)} + he^{\sqrt{\frac{hr}{8}}(x+y)}\frac{t^\alpha}{\Gamma(1+\alpha)}\\
+ h^2e^{\sqrt{\frac{hr}{8}}(x+y)}\frac{t^{2\alpha}}{\Gamma(1+2\alpha)}.
\end{aligned} \tag{49}
$$

Therefore, the n-th coefficient of $u(x,y,t)$ is

$$f_n(x,y) = h^n e^{\sqrt{\frac{hr}{8}}(x+y)}, \tag{50}$$

the n-th ERPSM approximate solutions of $u(x,y,t)$ is

$$u_n(x,y,t) = e^{\sqrt{\frac{hr}{8}}(x+y)}\sum_{n=0}^{i}\frac{(ht^\alpha)^n}{\Gamma(1+n\alpha)}, \tag{51}$$

and as $n \to \infty$ we have

$$u(x,y,t) = lim_{n\to\infty}u_n(x,y,t) = e^{\sqrt{\frac{hr}{8}}(x+y)}E_\alpha(ht^\alpha), \tag{52}$$

For $\alpha \to 1$, we have $E_\alpha(z) = e^{ht}$ and hence $e^{\sqrt{\frac{hr}{8}}(x+y)+ht}$ is the exact solution of the standard partial time-derivative of (39).

In Fig. 3, we obtain the 3D graphics of the approximate solutions and exact solutions by Matlab 2018b Windows(64 bit). The approximate solutions are the same as the exact solutions. The parameters in Fig. 3 are $\alpha = 1, t = 1, h = 1, r = 2$, where Fig. 3(a) represents the exact solutions and Fig. 3(b) represents the approximate solutions.

In Tab. 3, we present the comparison of the absolute errors for the obtained results and the exact solution by the ERPSM when $h = 1, r = 2$.

In Tab. 3, absolute errors increases as t increases when x, y are unchanged, absolute errors increases as x, y increases when t is unchanged.

When $\alpha = 0.1, 0.3, 0.5, 0.7, 0.9$, linear independence can be verified by using the ERPSM. Then, we use the Elzaki transform method to attain the unknown coefficients.

In Fig. 4, pictures show the impact of different α and x, y when $h = 1, r = 2$, $t \in [0,1], x \in (0,10], y \in (0,10]$ on the $|\tilde{Res}_2(x,y,t)|$. We list four cases of fixed x, y to observe the variation of $|\tilde{Res}_2(x,y,t)|$ in each subplot with different α and t. Different colors and line shapes represent different α. Fig. 4(a)-4(d) respectively show $|\tilde{Res}_2(x,y,t)|$ of x, y are fixed values of 10, 1, 0.1 and 0.01.

We can draw a conclusion from Fig. 4 that $|\tilde{Res}_2(x,y,t)|$ decreases as the constants x, y decreases when α and t are unchanged. Besides, $|\tilde{Res}_2(x,y,t)|$ decreases as α increases when t and x, y are unchanged, $|\tilde{Res}_2(x,y,t)|$ increases as $t \in (0,1)$ increases when α and x, y are unchanged.

Remark 1. In Example 2, when $t = 0$, the values of the y-axis in Figure 4 do not start at zero. The approximate solutions only have three items, which results in some errors.

$$\begin{aligned}&|Res_2(x,y,t)|\\&=|D_t^\alpha u_2(x,y,t)-(u_2^2(x,y,t))_{xx}-(u_2^2(x,y,t))_{yy}\\&-hu_2(x,y,t)(1-ru_2(x,y,t))|\\&=|f_1(x,y)+f_2(x,y)\frac{t^\alpha}{\Gamma(1+\alpha)}-((f_0(x,y)\\&+f_1(x,y)\frac{t^\alpha}{\Gamma(1+\alpha)}+f_2(x,y)\frac{t^{2\alpha}}{\Gamma(1+2\alpha)})^2)_{xx}\\&-((f_0(x,y)+f_1(x,y)\frac{t^\alpha}{\Gamma(1+\alpha)}+f_2(x,y)\frac{t^{2\alpha}}{\Gamma(1+2\alpha)})^2)_{yy}\\&-h(f_0(x,y)+f_1(x,y)\frac{t^\alpha}{\Gamma(1+\alpha)}+f_2(x,y)\frac{t^{2\alpha}}{\Gamma(1+2\alpha)})(1\\&-r(f_0(x,y)+f_1(x,y)\frac{t^\alpha}{\Gamma(1+\alpha)}+f_2(x,y)\frac{t^{2\alpha}}{\Gamma(1+2\alpha)}))|\\&=|he^{\sqrt{\frac{hr}{8}}(x+y)}+\frac{h^2e^{\sqrt{\frac{hr}{8}}(x+y)}t^\alpha}{\Gamma(1+\alpha)}-((e^{\sqrt{\frac{hr}{8}}(x+y)}\\&+\frac{he^{\sqrt{\frac{hr}{8}}(x+y)}t^\alpha}{\Gamma(1+\alpha)}+\frac{h^2e^{\sqrt{\frac{hr}{8}}(x+y)}t^{2\alpha}}{\Gamma(1+2\alpha)})^2)_{xx}-((e^{\sqrt{\frac{hr}{8}}(x+y)}\\&+\frac{he^{\sqrt{\frac{hr}{8}}(x+y)}t^\alpha}{\Gamma(1+\alpha)}+\frac{h^2e^{\sqrt{\frac{hr}{8}}(x+y)}t^{2\alpha}}{\Gamma(1+2\alpha)})^2)_{yy}\\&-h(e^{\sqrt{\frac{hr}{8}}(x+y)}+\frac{he^{\sqrt{\frac{hr}{8}}(x+y)}t^\alpha}{\Gamma(1+\alpha)}+\frac{h^2e^{\sqrt{\frac{hr}{8}}(x+y)}t^{2\alpha}}{\Gamma(1+2\alpha)})(1-\\&r(e^{\sqrt{\frac{hr}{8}}(x+y)}+\frac{he^{\sqrt{\frac{hr}{8}}(x+y)}t^\alpha}{\Gamma(1+\alpha)}+\frac{h^2e^{\sqrt{\frac{hr}{8}}(x+y)}t^{2\alpha}}{\Gamma(1+2\alpha)})|\end{aligned} \tag{53}$$

When $t=0$,

$$\begin{aligned}&|Res_2(x,y,t)|\\&=|he^{\sqrt{\frac{hr}{8}}(x+y)}-(e^{2\sqrt{\frac{hr}{8}}(x+y)})_{xx}-(e^{2\sqrt{\frac{hr}{8}}(x+y)})_{yy}\\&-he^{\sqrt{\frac{hr}{8}}(x+y)}+hre^{\sqrt{\frac{hr}{8}}(x+y)}|\\&=|hre^{\sqrt{\frac{hr}{8}}(x+y)}|\neq 0.\end{aligned} \tag{54}$$

Example 3 With $a=1, b=1, h=\frac{1}{96}$, and $r=48$, considering the following TFBPDEs

$$\begin{aligned}D_t^\alpha u(x,y,t)=&(u^2(x,y,t))_{xx}+(u^2(x,y,t))_{yy}\\&+\frac{1}{96}u^{-1}(x,y,t)-\frac{1}{2}, t>0, 0<\alpha\leq 1,\end{aligned} \tag{55}$$

with

$$u(x,y,t)|_{t=0}=\frac{1}{4}\sqrt{2(x^2+y^2)+y+5}, \tag{56}$$

and the exact solution when $\alpha=1$ is[3]

$$u(x,y,t)=\frac{1}{4}\sqrt{2(x^2+y^2)+y+\frac{t}{3}+5}. \tag{57}$$

Using Elzaki transform

$$\begin{aligned}E[D_t^\alpha u(x,y,t)]=&E[(u^2(x,y,t))_{xx}+(u^2(x,y,t))_{yy}\\&+\frac{1}{96}u^{-1}(x,y,t)-\frac{1}{2}],\end{aligned} \tag{58}$$

Applying the differentiation property of Elzaki transform and the initial conditions above, we can obtain

$$\begin{aligned}E[u(x,y,t)]=&g(x,y,t)+v^\alpha E[(u^2(x,y,t))_{xx}\\&+(u^2(x,y,t))_{yy}+\frac{1}{96}u^{-1}(x,y,t)-\frac{1}{2}].\end{aligned} \tag{59}$$

Taking Elzaki inverse

$$\begin{aligned}u(x,y,t)=&G(x,y,t)+E^{-1}[v^\alpha E[(u^2(x,y,t))_{xx}\\&+(u^2(x,y,t))_{yy}+\frac{1}{96}u^{-1}(x,y,t)-\frac{1}{2}]].\end{aligned} \tag{60}$$

We use the classic RPSM. The form of $u_i(x,y,t)$ can be written as

$$S_i=\sum_{n=0}^{i}u_n(x,y,t)=\sum_{n=0}^{i}f_n(x,y)\frac{t^{n\alpha}}{\Gamma(1+n\alpha)}. \tag{61}$$

Then, we find the solution of $f_n(x,y)$ by

$$\begin{aligned}Res_i(x,y,t)=&u_i(x,y,t)-\{G(x,y,t)\\&+E^{-1}[v^\alpha E[(u_{i-1}^2(x,y,t))_{xx}+(u_{i-1}^2(x,y,t))_{yy}\\&+\frac{1}{96}u_{i-1}^{-1}(x,y,t)-\frac{1}{2}]]\}.\end{aligned} \tag{62}$$

When $i=0$

$$Res_0(x,y,t)=u_0(x,y,t)-G(x,y,t),$$

and from the equation (17), we have

$$u_0(x,y,t)=f_0(x,y),$$

from formula (19), we have $Res_0(x,y,t)|_{t=0}=0$, thus

$$f_0(x,y)=\frac{1}{4}\sqrt{2(x^2+y^2)+y+5}. \tag{63}$$

When $i=1$

$$\begin{aligned}Res_1(x,y,t)=&u_1(x,y,t)-\{G(x,y,t)+E^{-1}[v^\alpha E[\\&(u_0^2(x,y,t))_{xx}+(u_0^2(x,y,t))_{yy}+\frac{1}{96}u_0^{-1}(x,y,t)-\frac{1}{2}]]\},\end{aligned}$$

with the condition

$$u_1(x,y,t)=f_0(x,y)+f_1(x,y)\frac{t^\alpha}{\Gamma(1+\alpha)},$$

Then, we can attain

$$\begin{aligned}&Res_1(x,y,t)\\&=f_0(x,y)+f_1(x,y)\frac{t^\alpha}{\Gamma(1+\alpha)}-\{G(x,y,t)+E^{-1}[v^\alpha E[\\&(f_0^2(x,y))_{xx}+(f_0^2(x,y))_{yy}+\frac{1}{96}f_0^{-1}(x,y)-\frac{1}{2}]]\}\\&=f_1(x,y)\frac{t^\alpha}{\Gamma(1+\alpha)}-E^{-1}[v^\alpha E[\frac{1}{24\sqrt{2(x^2+y^2)+y+5}}]]\\&=f_1(x,y)\frac{t^\alpha}{\Gamma(1+\alpha)}-E^{-1}[\frac{1}{24\sqrt{2(x^2+y^2)+y+5}}v^{\alpha+2}]\\&=f_1(x,y)\frac{t^\alpha}{\Gamma(1+\alpha)}-\frac{\frac{1}{24\sqrt{2(x^2+y^2)+y+5}}t^\alpha}{\Gamma(1+\alpha)},\end{aligned}$$

Then, we solve $t^{-\alpha}Res_1(x,y,t)|_{t=0}=0$ to obtain

$$f_1(x,y)=\frac{1}{24\sqrt{2(x^2+y^2)+y+5}}. \tag{64}$$

When $i=2$

$$\begin{aligned}Res_2(x,y,t)=&u_2(x,y,t)-\{G(x,y,t)+E^{-1}[v^\alpha E[\\&(u_1^2(x,y,t))_{xx}+(u_1^2(x,y,t))_{yy}+\frac{1}{96}u_1^{-1}(x,y,t)-\frac{1}{2}]]\},\end{aligned}$$

with the condition

$$u_2(x,y,t)=f_0(x,y)+f_1(x,y)\frac{t^\alpha}{\Gamma(1+\alpha)}+f_2(x,y)\frac{t^{2\alpha}}{\Gamma(1+2\alpha)},$$

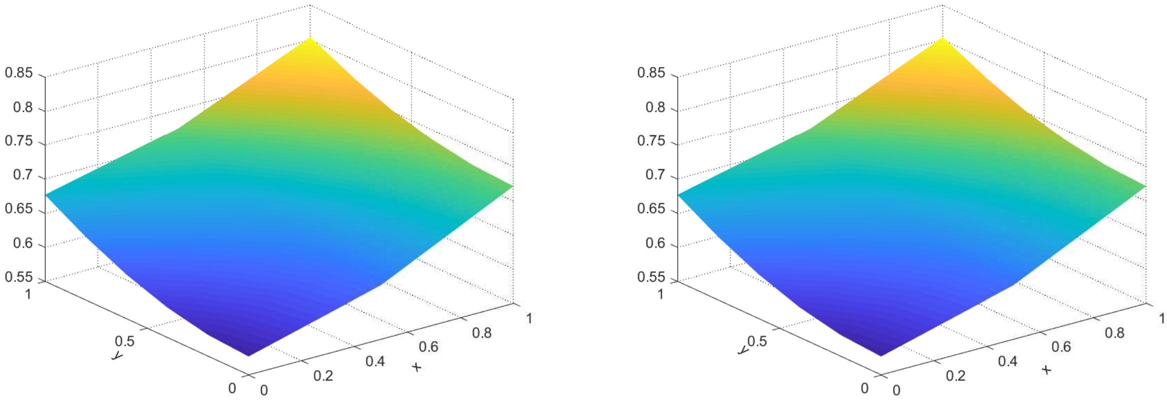

(a) $u(x,y,t)_{exact}$

(b) $u(x,y,t)_{ERPSM}$

Fig. 5: 3D graphics of exact and approximate solutions(Ex. 3.)

Then, we can get

$$
\begin{aligned}
&Res_2(x,y,t)\\
&=f_0(x,y)+f_1(x,y)\frac{t^{\alpha}}{\Gamma(1+\alpha)}+f_2(x,y)\frac{t^{2\alpha}}{\Gamma(1+2\alpha)}-\{G(x,y,t)\\
&+E^{-1}[v^{\alpha}E[((f_0(x,y)+f_1(x,y)\frac{t^{\alpha}}{\Gamma(1+\alpha)})^2)_{xx}+((f_0(x,y)\\
&+f_1(x,y)\frac{t^{\alpha}}{\Gamma(1+\alpha)})^2)_{yy}+\frac{1}{96}(f_0(x,y)+f_1(x,y)\frac{t^{\alpha}}{\Gamma(1+\alpha)})^{-1}-\frac{1}{2}]]\}\\
&=f_1(x,y)\frac{t^{\alpha}}{\Gamma(1+\alpha)}+f_2(x,y)\frac{t^{2\alpha}}{\Gamma(1+2\alpha)}-\\
&E^{-1}[v^{\alpha}E[\frac{1}{24\sqrt{2(x^2+y^2)}+y+5}]]\\
&-E^{-1}[v^{\alpha}E[-\frac{1}{144(\sqrt{2(x^2+y^2)}+y+5)^3}]]-E^{-1}[v^{\alpha}E[\\
&\frac{2(5308416x^2+2(2304y+576)^2-5308416y^2-2654208y-13271040)}{\alpha!(1152x^2+1152y^2+576y+2880)^3}]]\\
&=f_1(x,y)\frac{t^{\alpha}}{\Gamma(1+\alpha)}+f_2(x,y)\frac{t^{2\alpha}}{\Gamma(1+2\alpha)}\\
&-E^{-1}[\frac{1}{24\sqrt{2(x^2+y^2)}+y+5}v^{\alpha+2}]\\
&-E^{-1}[-\frac{1}{144(\sqrt{2(x^2+y^2)}+y+5)^3}v^{2\alpha+2}]-E^{-1}\\
&[\frac{2(5308416x^2+2(2304y+576)^2-5308416y^2-2654208y-13271040)}{\alpha!(1152x^2+1152y^2+576y+2880)^3}\\
&v^{3\alpha+2}]\\
&=f_1(x,y)\frac{t^{\alpha}}{\Gamma(1+\alpha)}+f_2(x,y)\frac{t^{2\alpha}}{\Gamma(1+2\alpha)}-\frac{\frac{1}{24\sqrt{2(x^2+y^2)+y+5}}t^{\alpha}}{\Gamma(1+\alpha)}\\
&-\frac{\frac{1}{-144(\sqrt{2(x^2+y^2)+y+5})^3}t^{2\alpha}}{\Gamma(1+2\alpha)}\\
&-\frac{\frac{2(5308416x^2+2(2304y+576)^2-5308416y^2-2654208y-13271040)}{\alpha!(1152x^2+1152y^2+576y+2880)^3}t^{3\alpha}}{\Gamma(1+3\alpha)},
\end{aligned}
$$

Then, divide by $t^{2\alpha}$ on both sides of $Res_2(x,y,t)$ and make t as zero, we can obtain

$$
f_2(x,y)=-\frac{1}{144(\sqrt{2(x^2+y^2)}+y+5)^3}. \tag{65}
$$

We can get an approximate result

$$
\begin{aligned}
u_2(x,y,t)=&\frac{1}{4}\sqrt{2(x^2+y^2)+y+5}\\
&+\frac{1}{24\sqrt{2(x^2+y^2)+y+5}}\frac{t^{\alpha}}{\Gamma(1+\alpha)}\\
&-\frac{1}{144(\sqrt{2(x^2+y^2)+y+5})^3}\frac{t^{2\alpha}}{\Gamma(1+2\alpha)}.
\end{aligned} \tag{66}
$$

In Fig. 5, we obtain the 3D graphics of the approximate solutions and exact solutions by Matlab 2018b Windows(64 bit). The approximate solutions are the same as the exact solutions. The parameters in Fig. 5 are $\alpha = 1, t = 1$, where Fig. 5(a) represents the exact solutions and Fig. 5(b) represents the approximate solutions.

In Tab. 4 and Tab. 5, the absolute error of three methods are calculated when $t = 10$ and $t = 20$. The three methods are the ERPSM, the VIM[4] and the ADM[4]. Besides, the ERPSM is denoted by $u_i(x,y,t)$, the VIM and ADM are denoted by $\tilde{u}_i(x,y,t)$.

In Tab. 4, we can get the absolute errors range between $10^{-3}$and 10^{-16}. And from Tab. 5, the absolute errors range between 10^{-2} and 10^{-15}. Under the same conditions, the results of ERPSM, VIM and ADM are the same, the new method requires less computation, and the results are more accurate.

When $\alpha = 0.1, 0.3, 0.5, 0.7, 0.9$, linear independence can be verified by using the ERPSM. Then, we use the Elzaki transform method to attain the unknown coefficients.

In Fig. 6, pictures show the effect of different α and x, y when $t \in [0,1], x \in (0,10], y \in (0,10]$ on the $|\tilde{Res}_2(x,y,t)|$. We list four cases of fixed x, y to observe the variation of $|\tilde{Res}_2(x,y,t)|$ in each subplot with different α and t. Different colors and line shapes represent different α. Figures 6(a)-6(d) respectively show $|\tilde{Res}_2(x,y,t)|$ of x, y are fixed values of 10, 1, 0.1 and 0.01.

We can draw a conclusion from Fig. 6 that $|\tilde{Res}_2(x,y,t)|$ increases as the constants x, y decreases when α and t are unchanged. Besides, $|\tilde{Res}_2(x,y,t)|$ decreases as α increases when t and x, y are unchanged, $|\tilde{Res}_2(x,y,t)|$ increases as $t \in (0,1)$ increases when α and x, y are unchanged.

TABLE IV: Absolute errors by ERPSM, VIM, ADM for $\alpha = 1, t = 10$(Ex. 3.)

(x,y)	$u(x,y,t)_{exact}$	$u_i(x,y,t)_{i=2}^{ERPSM}$	$\tilde{u}_i(x,y,t)_{i=2}^{VIM}$[4]	$\tilde{u}_i(x,y,t)_{i=2}^{ADM}$[4]	$Error(x,y,t)_{i=2}^{ERPSM}$	$Error(x,y,t)_{i=2}^{VIM}$[4]	$Error(x,y,t)_{i=2}^{ADM}$[4]
(-450,-450)	224.938649	224.938649	224.938649	224.938652	9.813846×10^{-16}	7.272155×10^{-12}	2.573384×10^{-6}
(-400,-400)	199.938793	199.938793	199.938793	199.938796	1.768786×10^{-15}	1.106995×10^{-12}	3.257144×10^{-6}
(-300,-300)	149.939224	149.939224	149.939224	149.939230	7.457402×10^{-15}	3.578650×10^{-11}	5.791548×10^{-6}
(-250,-250)	124.939569	124.939569	124.939569	124.939577	1.856381×10^{-14}	7.431441×10^{-12}	8.341020×10^{-6}
(0,0)	0.721688	0.714299	0.543911	-0.087784	7.388344×10^{-3}	1.777776×10^{-1}	8.094717×10^{-1}
(50,50)	25.072811	25.072811	25.072811	25.073018	5.707042×10^{-11}	4.572776×10^{-8}	2.068923×10^{-4}
(100,100)	50.067663	50.067663	50.067663	50.067714	1.796542×10^{-12}	2.877083×10^{-9}	5.192803×10^{-5}
(200,200)	100.065083	100.065083	100.065083	100.065096	5.633268×10^{-14}	1.803953×10^{-10}	1.300298×10^{-5}
(350,350)	175.063976	175.063976	175.063976	175.063981	3.436987×10^{-15}	1.906919×10^{-11}	4.248496×10^{-6}
(500,500)	250.063534	250.063534	250.063534	250.063536	5.779725×10^{-16}	4.562573×10^{-12}	2.082251×10^{-6}

TABLE V: Absolute errors by ERPSM, VIM, ADM for $\alpha = 1, t = 20$(Ex. 3.)

(x,y)	$u(x,y,t)_{exact}$	$u_i(x,y,t)_{i=2}^{ERPSM}$	$\tilde{u}_i(x,y,t)_{i=2}^{VIM}$[4]	$\tilde{u}_i(x,y,t)_{i=2}^{ADM}$[4]	$Error(x,y,t)_{i=2}^{ERPSM}$	$Error(x,y,t)_{i=2}^{VIM}$[4]	$Error(x,y,t)_{i=2}^{ADM}$[4]
(-450,-450)	224.939112	224.939112	224.939112	224.939122	7.851057×10^{-15}	7.272155×10^{-12}	1.029354×10^{-5}
(-400,-400)	199.939314	199.939314	199.939314	199.939327	1.415024×10^{-14}	1.106995×10^{-11}	2.316619×10^{-5}
(-300,-300)	149.939919	149.939919	149.939916	149.939942	5.965887×10^{-14}	3.578650×10^{-11}	2.316619×10^{-5}
(-250,-250)	124.940402	124.940402	124.940402	124.940436	1.485093×10^{-13}	7.431441×10^{-11}	3.336408×10^{-5}
(0,0)	0.853913	0.807469	-0.562830	-2.400864	4.644357×10^{-2}	1.777776×10^{-1}	3.254777
(50,50)	25.076965	25.076965	25.076965	25.077792	4.564688×10^{-10}	3.658223×10^{-7}	8.275692×10^{-4}
(100,100)	50.069743	50.069743	50.069743	50.069951	1.437159×10^{-11}	2.301665×10^{-8}	2.077121×10^{-4}
(200,200)	100.066124	100.066124	100.066124	100.066176	4.506556×10^{-13}	1.442949×10^{-9}	5.201194×10^{-5}
(350,350)	175.064571	175.064571	175.064571	175.064588	2.749578×10^{-14}	1.538449×10^{-10}	1.699398×10^{-5}
(500,500)	250.063950	250.064817	250.063950	250.063958	4.623771×10^{-14}	3.683809×10^{-11}	8.329005×10^{-6}

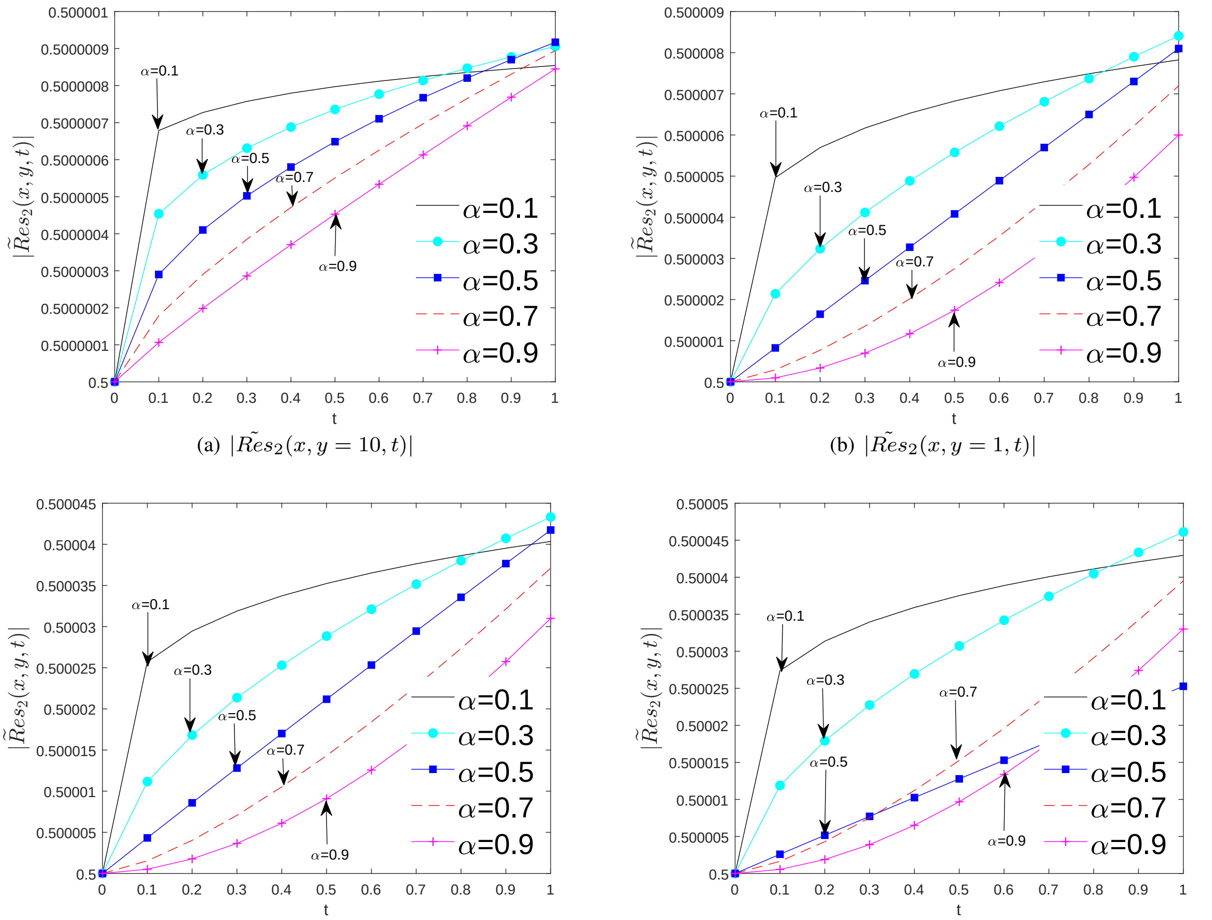

(a) $|\tilde{Res}_2(x, y = 10, t)|$ (b) $|\tilde{Res}_2(x, y = 1, t)|$

(c) $|\tilde{Res}_2(x, y = 0.1, t)|$ (d) $|\tilde{Res}_2(x, y = 0.01, t)|$

Fig. 6: $|\tilde{Res}_2(x, y, t)|$ with different t and α(Ex. 3.)

V. Conclusion

In this article, we beneficially applied the ERPSM to find the approximate solutions for TFBPDEs. This new method combines the Elzaki transform with the RPSM, which is an improvement on the classic RPSM. We obtain more accurate approximate solutions with less calculation and small error. The final results of the approximate solution we present in tables and pictures. In conclusion, ERPSM provides a simple and accurate algorithm for finding approximate solutions of the TFBPDEs.

References

[1] Q. Yang, D. Chen, T. Zhao, Y.Q. Chen, "Fractional calculus in image processing: a review," *Fractional Calculus & Applied Analysis*, vol. 19, no. 10, pp. 1222-1249, 2016.

[2] R. Metzler, J. Klafter, "The random walk's guide to anomalous diffusion: a fractional dynamics approach," *Physics Reports*, vol. 339, no. 1, pp. 1-77, 2000.

[3] S. O. Edeki, I. Adinya, O. O. Ugbebor, "The Effect of Stochastic Capital Reserve on Actuarial Risk Analysis via an Integro-differential Equation," *IAENG International Journal of Applied Mathematics*, vol. 44, no. 2, pp. 83-90, 2014.

[4] F. Shakeri, M. Dehghan, "Numerical solution of a biological population model using He's variational iteration method," *Computers & Mathematics with Applications*, vol. 54, no. 7, pp. 1197-1209, 2007.

[5] S.S. Ray, "Analytical solution for the space fractional diffusion equation by two-step Adomian Decomposition Method," *Communications in Nonlinear ence and Numerical Simulation*, vol. 14, no. 4, pp. 1295-1306, 2009.

[6] Y. Liu, Z. Li, Y. Zhang, "Homotopy perturbation method to fractional biological population equation," *Fractional Differential Calculus*, vol. 1, no. 1, pp. 117-124, 2011.

[7] A. Khalouta, A. Kadem, "A new numerical technique for solving Caputo time-fractional biological population equation," *AIMS Mathematics*, vol. 4, no. 5, pp. 1307-1319, 2019.

[8] S. O. Edeki , O. O. Ugbebor, E. A. Owoloko, "Analytical Solution of the Time-fractional Order Black-Scholes Model for Stock Option Valuation on No Dividend Yield Basis," *IAENG International Journal of Applied Mathematics*, vol. 47, no. 4, pp. 407-416, 2017.

[9] P. Amit, G. Manish, G. Shivangi, "Fractional variational iteration method for solving time-fractional Newell-Whitehead-Segel equation," *Nonlinear Engineering*, vol. 8, no. 1, pp. 164-171, 2019.

[10] M. Alquran, "Analytical solutions of fractional foam drainage equation by residual power series method," *Mathematical Sciences*, vol. 8, no. 4, pp. 153-160, 2014.

[11] M. Alquran, H.M. Jaradat, M.I. Syam, "Analytical solution of the time-fractional Phi-4 equation by using modified residual power series method," *Nonlinear Dynamics*, vol. 90, no. 4, pp. 2525-2529, 2017.

[12] I. Komashynska, M.A. Smadi, O.A. Arqub, S. Momani, "An efficient analytical method for solving singular initial value problems of nonlinear systems," *Applied Mathematics & Information ences*, vol. 10, no. 2, pp. 647-656, 2016.

[13] S. Kumar, A. Kumar, D. Baleanu, "Two analytical methods for time-fractional nonlinear coupled Boussinesq-Burger's equations arise in propagation of shallow water waves," *Nonlinear Dynamics*, vol. 85, no. 2, pp. 699-715, 2016.

[14] H.M. Jaradat, S. Al-Shar'a, Q.J.A. Khan, M. Alquran, K. Al-Khaled, "Analytical Solution of Time-Fractional Drinfeld-Sokolov-Wilson System Using Residual Power Series Method," *IAENG International Journal of Applied Mathematics*, vol. 46, no.1, pp. 64-70, 2016.

[15] S.M. Momani, O.A. Arqub, M.A. Hammad, Z.A. Hammour, "A Residual Power Series Technique for Solving Systems of Initial Value Problems," *Applied Mathematics & Information ences*, vol. 10, no. 2, pp. 765-775, 2017.

[16] S. Mehmet, A. Marwan, D.K. Hamed, "On the comparison of perturbation-iteration algorithm and residual power series method to solve fractional Zakharov-Kuznetsov equation," *Results in Physics*, vol. 9, pp. 321-327, 2018.

[17] M.A. Qurashi, Z. Korpinar, D. Baleanu, M. Inc, "A new iterative algorithm on the time-fractional Fisher equation: Residual power series method," *Advances in Mechanical Engineering*, vol. 9, no. 9, pp. 1-8, 2007.

[18] A. Kumar, S. Kumar, "Residual power series method for fractional Burger types equations," *Nonlinear Engineering*, vol. 5, no. 4, pp. 235-244, 2016.

[19] A.K.H. Sedeeg, "A Coupling Elzaki Transform and Homotopy Perturbation Method for Solving Nonlinear Fractional Heat-Like Equations," *American Journal of Mathematical & Computer Modelling*, vol. 1, no. 1, pp. 15-20, 2016.

[20] R.M. Jena, S. Chakraverty, "Solving time-fractional NavierStokes equations using homotopy perturbation Elzaki transform," *SN Applied Sciences*, vol. 1, no. 1, pp. 1-13, 2019.

[21] T.M. Elzaki, E.M.A. Hilal, "Solution of Linear and Nonlinear Partial Differential Equations Using Mixture of Elzaki Transform and the Projected Differential Transform Method," *Mathematical Theory and Modeling*, vol. 2, no. 4, pp. 50-59, 2012.

[22] D. Baleanu, K. Diethelm, E. Scalas, J. Trujillo, "Fractional Calculus: Models and Numerical Methods," *World Scientific*, 2012.

[23] E. Keshavarz, Y. Ordokhani, M. Razzaghi, "Bernoulli wavelet operational matrix of fractional order integration and its applications in solving the fractional order differential equations," *Applied Mathematical Modelling*, vol. 38, pp. 6038-6051, 2014.

[24] P. Rahimkhani, Y. Ordokhani, E. Babolian, "Numerical solution of fractional pantograph differential equations by using generalized fractional-order Bernoulli wavelet," *Journal of Computational and Applied Mathematics*, vol. 309, pp. 493-510, 2016.

[25] A. El-Ajou, O.A. Arqub, S. Momani, "Approximate analytical solution of the nonlinear fractional KdVBurgers equation: A new iterative algorithm," *Journal of Computational Physics*, vol. 293, pp. 81-95, 2015.

[26] T.M. Elzaki, "The New Integral Transform "ELzaki Transform"," *Global Journal of Pure and Applied Mathematics*, vol. 7, no. 1, pp. 57-64, 2011.

[27] M. Suleman, T.M. Elzaki, Q. Wu, N. Anjum, J.U. Rahman, "New Application of Elzaki Projected Differential Transform Method," *Journal of Computational and Theoretical Nanoscience*, vol. 14, no. 1, pp. 631-639, 2017.

[28] M. Alquran, K. Al-Khaled, J. Chattopadhyay, "Analytical solutions of fractional population diffusion model: Residual power series," *Nonlinear Studies*, vol. 22, no. 1, pp. 31-39, 2015.

[29] I. Podlubny, "Fractional Differential Equations: an Introduction to Fractional Derivatives, Fractional Differential Equations, to Methods of Their Solution and Some of Their Applications," *Academic Press New York*, 1999.

[30] J. Zhang, Z. Wei, L. Li, C. Zhou, "Least-Squares Residual Power Series Method for the Time-Fractional Differential Equations," *Complexity*, 2019.